ALOE VERA-LOADED GELATIN METHACRYLOYL HYDROGELS AS POTENTIAL BONE BIOMATERIALS

Carmen-Valentina NICOLAE[1], Iulia-Maria IORDACHE[2], Adela BANCIU[3], Izabela-Cristina STANCU[4]

This study reports the development of gelatin methacryloyl (GelMA) hydrogels loaded with aloe vera (AV) compounds as potential biomaterials for bone tissue regeneration. By incorporating lyophilized AV gel and commercially available AV powder into GelMA hydrogels, we aimed to leverage the synergistic bioactivity of AV components for comprehensive tissue regeneration. The effect of AV compounds addition to the GelMA network was investigated through gel fraction evaluation and rheological measurements. The results suggest that the formulations could meet the standards for the targeted application, while their rheological, network-forming and antibacterial properties are significantly influenced by the incorporation of lyophilized AV gel.

Keywords: *aloe vera*, gelatin methacryloyl, hydrogels, bone biomaterials.

1. Introduction

Aloe Vera Barbadensis Miller, commonly known as aloe vera (AV), is a fascinating natural resource with versatile properties, holding great promise for tissue regeneration [1]. Over the years, AV has been extensively used for its therapeutic properties in pharmaceutical applications (e.g., in the treatment of wounds, ulcer, diabetes, cancer, HIV, psoriasis and eczemas), in dentistry, in food applications (nutraceuticals and functional foods, edible coatings), as well as in cosmetic applications (sunburn lotions, moisturizers) [2].

The components of AV that are responsible for its rich bioactivity are mainly found within the inner part of the leaf, constituting the AV gel, including carbohydrates, minerals, proteins, lipids, phenols, vitamins and inorganic

[1] Eng., PhD candidate, Dept. of Bioresources and Polymer Science, Faculty of Chemical Engineering and Biotechnologies, Advanced Polymer Materials Group, National University of Science and Technology POLITEHNICA Bucharest, Romania, e-mail: carmen.nicolae@upb.ro

[2] M.Sc., Smart Biomaterials and Applications, Faculty of Medical Engineering, National University of Science and Technology POLITEHNICA Bucharest, Romania, e-mail: iulia26iordache@yahoo.ro

[3] Lecturer, Faculty of Medical Engineering, National University of Science and Technology POLITEHNICA Bucharest, Romania, e-mail: adela.banciu@upb.ro

[4] Prof., Dept. of Bioresources and Polymer Science, Faculty of Chemical Engineering and Biotechnologies, Advanced Polymer Materials Group, National University of Science and Technology POLITEHNICA Bucharest, Romania, e-mail: izabela.stancu@upb.ro

compounds [3]. These constituents have been associated with specific biological activities that could promote bone tissue regeneration. Acetylated glucomannan (acemannan, ACE) was identified as the primary polysaccharide in the composition of AV gel, being linked to some of the plant's numerous bioactive effects. This compound has been mostly studied for the regeneration of bone defects localized in the oral and maxillofacial areas. ACE was shown to induce osteogenic differentiation and mineralization [4], promote cell proliferation, enhance protein expression of vascular endothelial growth factor (VEGF) and bone morphogenetic protein (BMP) [5, 6]. In clinical studies, pristine ACE sponges determined new bone formation in sinus augmentation surgeries [7, 8], enhanced early bone healing rate of periapical defects after surgery [9] and increased bone density in the tooth socket after molar removal [10].

However, although over 75 bioactive ingredients were identified in the AV gel, the plant's therapeutic activity was attributed to their synergistic action, rather than to individual compounds [3]. AV gel was shown to increase cell viability and compatibility of osteoblast-like cells, osteogenic cell proliferation, BMP-2 and BMP-7 expression, enhance mineralization, osteogenesis and maturation of newly formed bone [11, 12]. Clinical studies on bone defects caused by periodontitis confirm that AV gel determined significant reduction of pocket depth, increased bone density, improved adhesion and bone regeneration [13]. In addition to the benefits of its main polysaccharide constituent, other components of AV gel have demonstrated bioactive effects that are crucial for complete bone tissue regeneration. For example, emodin determines an increase in osteogenic gene expression markers and enhancement of osteoblast differentiation from bone marrow stem cells (BMSCs) both in vitro and in vivo [14], inorganic compounds like calcium and phosphorus are essential for mineralization and could intervene the regulation of bone metabolism [15], while β-carotene attenuates intracellular reactive oxygen species production and increases bone density through inhibition of osteoclast differentiation [16]. Considering its numerous advantages, AV gel emerges as a promising biomaterial for bone regeneration applications.

Gelatin methacryloyl (GelMA) is a highly versatile polymeric platform, widely used in tissue engineering due to its favorable properties, as it combines the natural-origin gelatin backbone with the synthetic polymerizable unsaturated C=C group from the methacryloyl substituents. This enables facile and robust hydrogel network formation through photopolymerization, allowing the adjustment of its mechanical properties and degradability by tailoring the synthesis and crosslinking parameters. In bone tissue engineering and regeneration applications, GelMA hydrogels can provide a hydrated microenvironment similar to the extracellular matrix, as its structure contains the Arg-Gly-Asp (RGD) sequences, being shown to improve cell adhesion, proliferation, osteogenic differentiation, mineralization and vascularization, while being able to modulate cellular responses in accordance with its properties [17, 18]. It has been demonstrated that GelMA hydrogels

effectively support various cell types relevant to bone regeneration, with excellent cell viability both on their surface and when encapsulated within the matrix [19], while promoting osteogenic differentiation of mesenchymal stem cells (MSCs), bone MSCs and human MSCs [20-22]. The osteogenic effects of GelMA can be enhanced by combining it with other osteogenic materials, which can lead to improved mechanical properties and augmented potential in regenerating bone defects [23].

Aiming to harness the synergistic benefits of AV's rich biochemical composition, while capitalizing on the unique attributes of GelMA, we have developed GelMA hydrogels loaded with AV compounds. We evaluated their network forming properties and investigated their compositional characteristics. The rheological behavior of both precursors and hydrogels was observed. Further, the antibacterial activity of the obtained hydrogels was tested against *Escherichia coli* (*E. coli*) Gram-negative bacteria, in order to assess their potential to facilitate efficient bone tissue regeneration.

2. Materials and Methods

2.1. Materials

Pristine gelatin (Type B, supplied by SKW Bio-systems, Ghent, Belgium) was modified through acylation reaction with methacrylic anhydride (MAA, 2.000 ppm topanol A as inhibitor, 94%, Aldrich) using the protocol described by Van Den Bulcke et al. [24]. In brief, 10 g of porcine gelatin were solubilized in PBS (Sigma Aldrich) at 50°C, followed by gradually adding methacrylic anhydride under magnetic stirring. After 1 h, the reaction was quenched by dilution with PBS and the solution was dialyzed for 24 h against distilled water at 40°C and lyophilized. Irgacure-2959 (2-Hydroxy-4′-(2-hydroxyethoxy)-2-methylpropiophenone, Sigma Aldrich) was used to initiate photopolymerization, forming the GelMA hydrogel network. AV commercial powder was acquired from a local pharmacy, while AV gel and ACE were extracted in-house from organically cultivated mature AV plant leaves sourced from a local market.

2.2. AV gel and ACE extraction

AV gel, as well as ACE, were extracted from *Aloe Vera Barbadensis Miller* leaves. After being washed with distilled water and ethanol, the leaves were cut with a scalpel, separating the gel from the plant outer rind and sap. The gel was blended, obtaining a homogenous liquid that was either used for ACE extraction or filtered and lyophilized to a fibrous material. The extraction of AV gel and ACE is schematized in Fig. 1.

Part of the extracted AV gel was used for ACE extraction, based on a protocol adapted from Kumar et al [25]. In this regard, 10 ml gel were centrifuged at 9500 g, 4°C for 30 min, to separate the polysaccharide fractions from the insoluble fibrous material. The supernatant was isolated, and the polysaccharide was precipitated by adding 3:1 volumes of cold absolute ethanol and kept for 24h under gentle agitation. The precipitate was collected by centrifugation, resuspended in distilled water and lyophilized.

The structural analysis of the extracted products was conducted through attenuated total reflection (ATR) Fourier transform infrared (FTIR) spectroscopy using a Jasco FT/IR-4200 spectrometer equipped with a Specac Golden Gate ATR module with diamond crystal and sapphire head, at a resolution of 4 cm^{-1}, in the wavenumber range 4000-600 cm^{-1}.

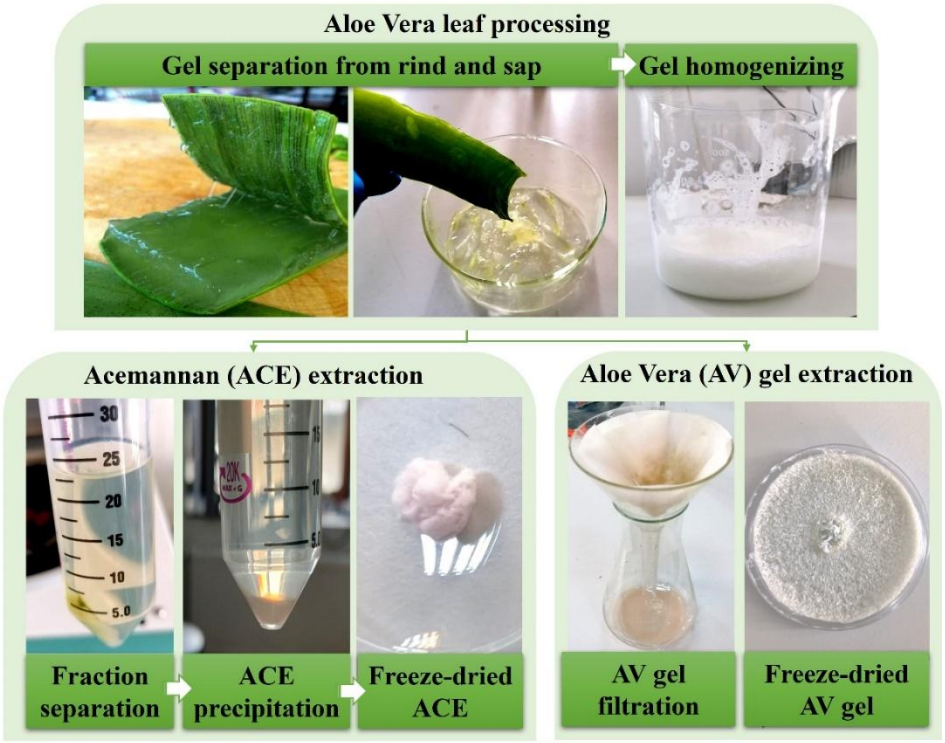

Fig. 1. *Aloe Vera Barbadensis Miller* leaf processing for extracting AV gel and ACE.

2.3. AV-loaded hydrogels fabrication

Three identical protein solutions were prepared by dissolving 10 g of GelMA in 10 ml sterile-filtered distilled water, kept at 40°C under magnetic stirring for 1h. Further, the 10% GelMA solutions were loaded with AV powder 1% (w/vol in the final solution) (GelMA/AV-P) and lyophilized AV gel 1% (w/vol) (GelMA/AV-L), keeping a control solution of pristine GelMA as well (GelMA/AV-

C). The compounds were incorporated by magnetic stirring for 1h, followed by the addition of 100 µl solution 10% w/v Irgacure-2959 in ethanol to each of the compositions and stirred in the dark until homogenous. Subsequently, the mixtures were poured into glass Petri dishes and photocrosslinked on a transilluminator (ECX-F26.M, Vilber), forming hydrogel networks with and without AV loading (Fig. 2).

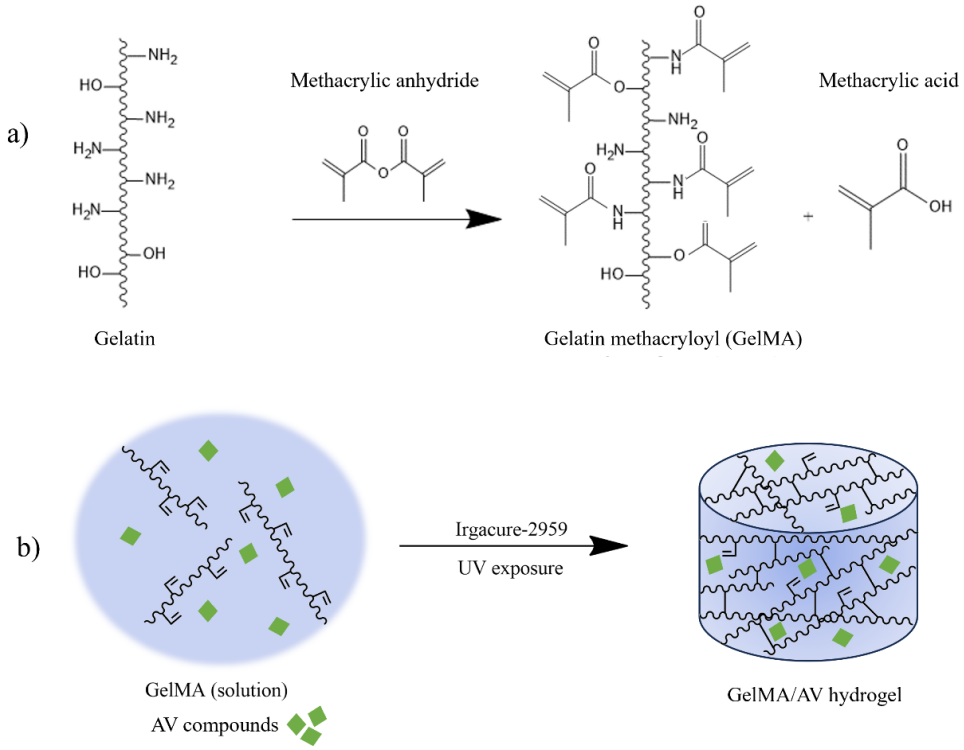

Fig. 2. Schematic representation of a) GelMA synthesis and b) GelMA/AV hydrogel formation through photocrosslinking.

2.6. AV-loaded hydrogels characterization

The crosslinking efficiency of the GelMA hydrogel network formation through photopolymerization was evaluated by gravimetrically estimating the gel fraction of the three types of hydrogels. Samples of 10 mm in diameter were cut, dried in the oven at 37°C overnight and weighed (Wi, initial weight). Further, the dry samples were incubated in distilled water, to remove water soluble fractions from the matrix. After 24h, they were dried and weighed (W_f, final weight). The gel fraction (GF, %) was determined using equation 1:

$$GF, \% = \frac{Wf}{Wi} * 100 \quad (1)$$

The influence of AV components on the ***rheological behavior*** of the AV/GelMA hydrogel precursors, as well as on the viscoelastic properties of the resulting hybrid hydrogels, was investigated using a rotational rheometer (Kinexus KNX2100, Malvern Instruments), equipped with plate-plate geometry and a solvent trap to prevent dehydration during testing. The hydrogel precursors viscosity was evaluated on a shear rate interval of 0.01-1000 s^{-1}, using a 0.5 mm gap. Hydrogel samples were hydrated by incubation at 37°C for 24h and cut using a 20 mm diameter metallic punch, matching the diameter of the upper plate. Using a plate-plate geometry with roughened surfaces to prevent hydrogel slipping, amplitude sweep tests were performed in a shear stress range of 0.01 to 1000 Pa, at a constant frequency of 1 Hz. From the linear viscoelastic region obtained from the amplitude sweep, we have determined a stress value of 1 Pa that was further used for subsequent frequency sweep tests, varying the frequency from 10 Hz to 0.1 Hz.

The ***structural evaluation*** of the hydrogels comprising GelMA, GelMA loaded with lyophilized AV gel, respectively with commercial AV powder, was performed by ATR-FTIR as described in 2.2.

The ***antibacterial effects*** of AV loading in GelMA-based hydrogels were evaluated against *Escherichia coli (E. coli)* Gram-negative bacteria, through Kirby-Bauer disk diffusion susceptibility method. Solid culture medium (Luria Bertani Agar, 2%) was used in a 100 mm diameter plaque, having a thickness of 4 mm. The inoculum was prepared in a liquid medium and after 6h of incubation, a turbidity equivalent to the 0.5 McFarland standard was obtained (0.125 optical density at 550 nm). The culture medium surface was inoculated by uniformly dispersing bacteria (1.5×10^8 CFU/ml) with a sterile swab. 6 mm wells were formed within the gel and the GelMA-AV samples were distributed on the plate with sterile tweezers. The inhibition zone was observed after incubation for 24h, under standard conditions (37°C and 5% CO_2).

The ***statistical analysis*** of the data was performed using GraphPad Prism 8.0, particularly one-way ANOVA tests coupled with Bonferroni's multiple comparisons test.

3. Results and discussion

In order to develop hydrogels loaded with AV for biomedical applications, we firstly assessed the extraction yield of AV components from organic leaves. Gravimetric measurements revealed that the obtained gel constitutes approximately 70% of the total leaf mass, while the purified polysaccharide, ACE, represents roughly only 0.05% of the leaf mass. The structure of the extracted AV gel and ACE was characterized using ATR-FTIR and compared with the spectrum of commercial AV-P (Fig. 3). Notably, the prominent wide band visible at 3600 cm^{-1} is primarily attributed to the stretching vibration of hydroxyl groups, while the peaks showing at 1578 cm^{-1} and 1421 cm^{-1} suggest the asymmetrical and

symmetrical stretching of the COO groups in carboxylate compounds of AV. Furthermore, the peak found at 870 cm^{-1} indicates the deformation of C-H bonds found in carbohydrate monomers [26]. The stretching of C=O bond can be observed by the peak showing at 1732 cm^{-1} (marked with black arrows), induced by the carbonyl groups found in AV compounds. The signal found at 1240 cm^{-1} may be attributed to the C-O-C stretching vibration of the acetyl groups, present in the polysaccharides structures and glucan units within the AV gel, in accordance with other studies [27].

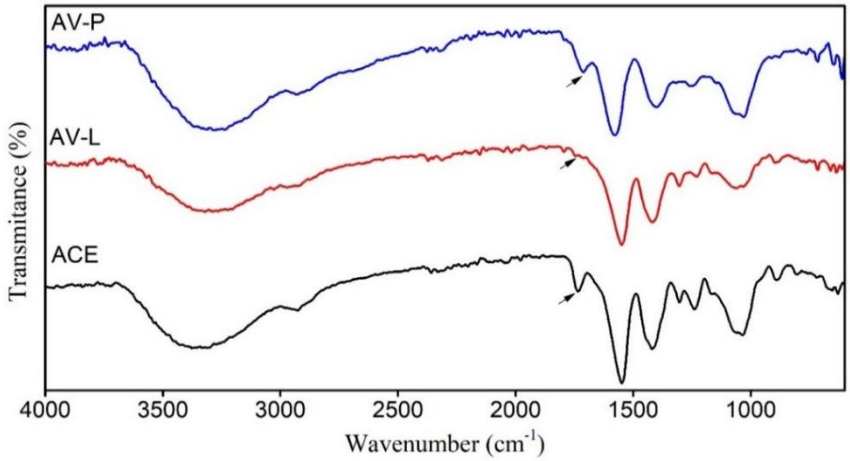

Fig. 3. Representative FTIR spectra for AV compounds: commercial AV powder (AV-P), extracted lyophilized AV gel (AV-L) and acemannan (ACE); arrows indicate the stretching vibration of C=O bond present in AV compounds.

The minimal extraction yield of ACE, the significant resource investment required for its extraction hindering scaled-up production of such hydrogels, as well as the proven synergistic activity of AV gel components led to using lyophilized AV gel rather than purified ACE for fabricating the composite hydrogels. Consequently, lyophilized AV gel and commercial AV powder were used to load GelMA hydrogels, forming three groups used for subsequent fabrication and testing: GelMA control hydrogel (GelMA/AV-C), GelMA hydrogel loaded with extracted lyophilized AV gel (GelMA/AV-L) and GelMA hydrogel loaded with commercial AV powder (GelMA/AV-P).

The ***crosslinking efficiency*** of the polymeric networks was evaluated gravimetrically, being weighed before and after 24h of incubation (Fig. 4). The gel fraction percentage indicates the crosslinked fraction within the hydrogel network, while the mass loss consists of soluble fractions and free polymer chains. The gel fraction was 84.59 ± 1.63 % for GelMA/AV-C, followed by 82.33 ± 4.57 % for GelMA/AV-P hydrogel. The difference between the control hydrogel and the sample loaded with AV powder is not statistically significant. However, for the hydrogel containing AV lyophilized gel, the gel fraction was 66.65 ± 2.87 %,

significantly different from both the pristine GelMA hydrogel and its powder-loaded counterpart ($p < 0.005$). This particularity could be attributed to the presence of larger pulp fibrous fragments from the lyophilized product, which may physically obstruct bond formation during the photopolymerization process, unlike the smaller AV particles present in the commercial AV powder.

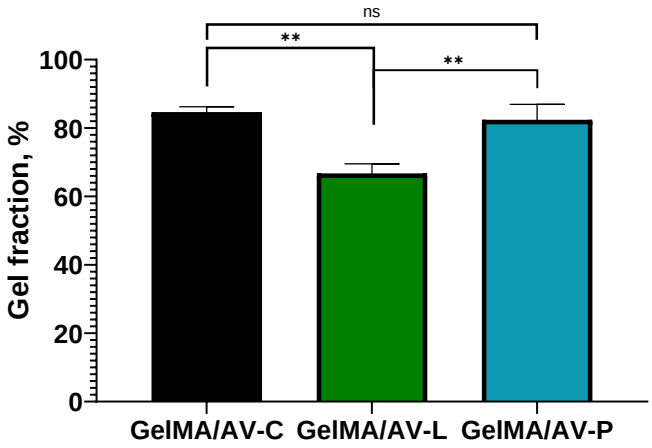

Fig. 4. Gel fraction of the hydrogel samples, indicating the crosslinking efficiency in the network formation process (** p=0.001, ns – not statistically significant).

The ***rheological behavior*** of the samples was evaluated both for the hydrogel precursors and on their crosslinked counterparts. The incorporation of extracted AV compounds impacts the rheological properties of the precursors, showing increased viscosity for the sample containing lyophilized AV gel (Fig. 5 a). The linear decrease in viscosity with increasing shear rate could be attributed to the possible alignment of AV fibers. Similar behavior can be observed in the case of fibrous cellulose [28] or clays [29], showing a tendency to align under shearing. In contrast, the addition of commercial AV powder had minimal influence on the precursor viscosity, exhibiting a similar behavior to pristine GelMA throughout the tested shear rate interval, possibly due to the reduced size of the powder granules.

The rheological analysis revealed distinct behavior among different hydrogel samples as well. For the control hydrogel, G' dominates over G" in the frequency interval of 1-10 Hz, with the decrease of over 100 Pa indicating a strong dependency on frequency, and possible destruction of the covalent network during the dynamic testing (Fig. 5 b). Furthermore, a cross-over of the two parameters may be observed, suggesting that the control hydrogel is not adequate for applications in a dynamic environment. Similar results for hydrogels consisting of 10% GelMA have been shown to be particularly effective for bone regeneration, promoting osteogenic differentiation in bioprinted constructs with dental pulp stem cells (DPSCs) [30]. The presence of AV compounds has a major impact on the

hydrogels' elastic properties. Both GelMA/AV-P and GelMA/AV-L exhibit a gel-like behavior on the entire frequency range (Fig. 5 c, d). GelMA/AV-L showed a slight dependency on the frequency above 1 Hz. Moreover, the values for both G' and G" are higher in the case of GelMA/AV-P when compared to GelMA/AV-L, possibly due to differences in compound assembly (powder vs. lyophilized gel). The oscillations present within the representative curves suggest to hydrogel slippage between rheometer plates, likely due to their increased water content after 24 h hydration.

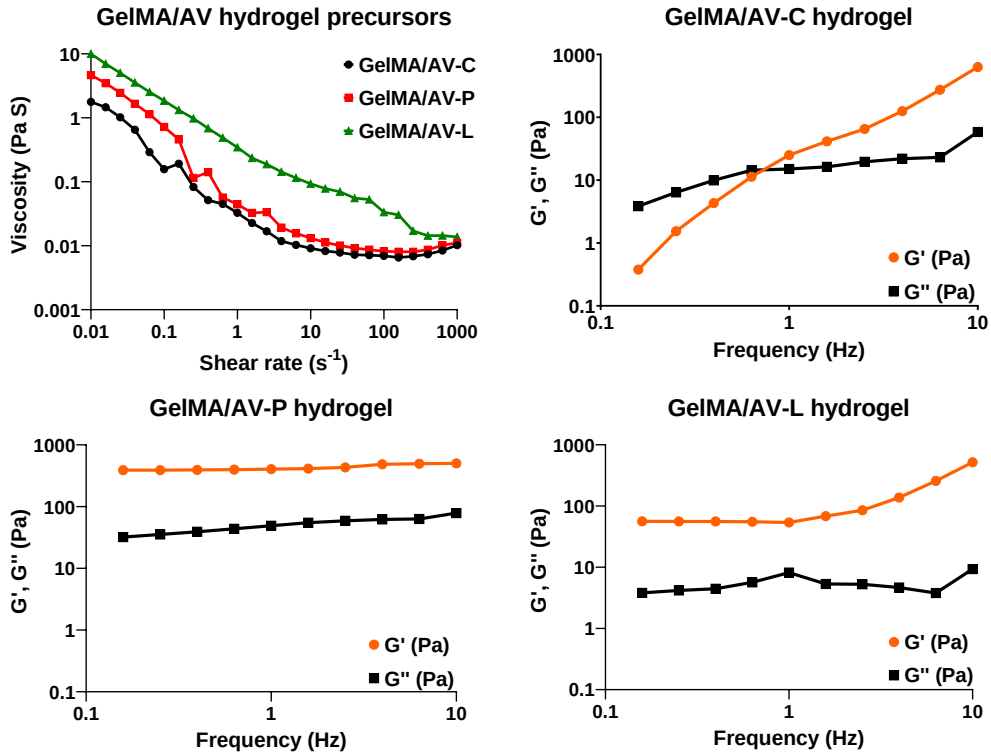

Fig. 5. Representative rheological behavior of the developed a) hydrogel precursors and hydrogels: b) GelMA/AV-C, c) GelMA/AV-P, d) GelMA/AV-L.

The ***ATR-FTIR spectra*** of pristine GelMA and of the fabricated hydrogels confirm the presence of protein- and polysaccharide-specific functional groups (Fig. 6). The representative spectra of raw GelMA exhibits characteristic bands for proteins, including the broad peak centered at 3290 cm^{-1} assigned to amide A [31]. This specific band indicates the overlapping stretching vibrations of O-H and N-H bonds, typical for amino acid residues in proteins. The shape of this wide band in GelMA is particular, comprised of a wider base, a narrow apex and a smaller peak marked with black arrows, located at 3523 cm^{-1}. Similarly, a broad band centered at 3301 cm^{-1} assigned to O-H is noticed in the spectra of carbohydrate structural

units in the structure of AV compounds. Consequently, for the composite hydrogels, numerous signals have dual origins, such as the band within the range of 3600-3000 cm^{-1} indicative of the O-H and N-H signals from aromatic amino acids in the structure of GelMA overlapping with the signals from O-H groups originating from carbohydrate monomers. In addition, the peak found at 3075 cm^{-1}, which can be attributed to C-H stretching vibration from the aromatic ring of tryptophan and phenyl-alanine in GelMA structure, can be observed in all spectra. (marked with black arrows). The peak at 1798 cm^{-1} can be attributed to the vibration of C=O in carbohydrate monomers (marked with black arrows), while its low intensity suggests the low content of AV compounds loading, as the GelMA matrix signals dominate the spectra of the composite hydrogels.

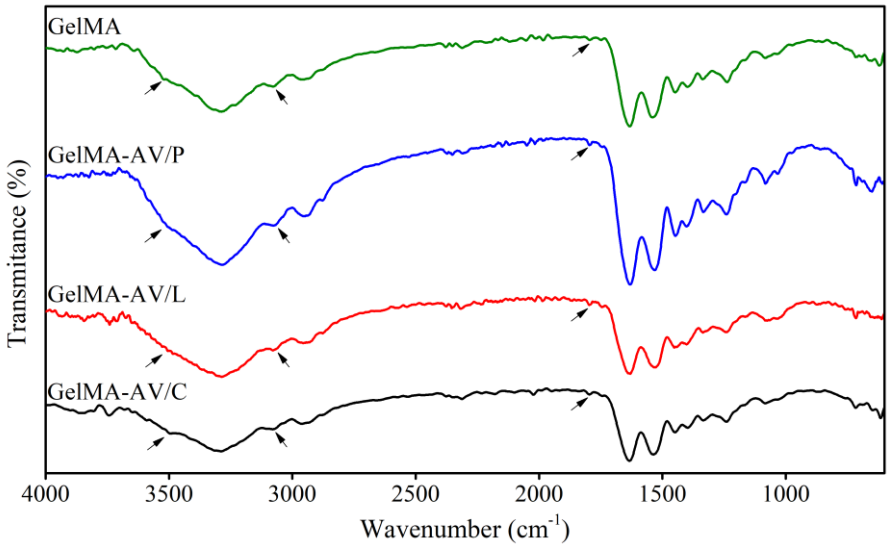

Fig. 6. Compositional characteristics of pristine GelMA and the developed hydrogels: commercial AV powder-loaded hydrogel (GelMA/AV-P), lyophilized AV gel-loaded hydrogel (GelMA/AV-L) and GelMA control hydrogel (GelMA/AV-C). Arrows indicate characteristic peaks of GelMA (overlapping O-H and N-H bond vibration at 3523 cm^{-1}, C-H stretching within aromatic rings at 3075 cm^{-1}) and AV compounds (C=O bond of carbohydrate monomers at 1798 cm^{-1}).

Common features across all samples include the peak at 1632 cm^{-1}, marking the amide I band, representative for C=O stretching, followed by a smaller peak at 1535 cm^{-1} corresponding to amide II band (N-H bending vibration and C-N stretching) [32]. The signal for N-H deformation, C-N stretching vibration and C=O bend of amide III band is observed at 1241 cm^{-1} [31]. The saturated C-H stretching vibration of $-CH_2$ groups can be observed at 2950 cm^{-1} (asymmetric stretching) and at 2875 cm^{-1} (symmetric stretching), while the bending vibrations of the same group can be located at 1449 cm^{-1} and 1338 cm^{-1} [33]. The ATR-FTIR measurements

validate the effective incorporation of AV, evidenced through the changes in shape of the broad band in the wavelength region of 3600-3300 cm^{-1}. Moreover, a subtle widening of this peak is observed in the case of AV-containing hydrogels, as well as an increase in intensity, which can be assigned to both the presence of numerous O-H groups found in the carbohydrate macromolecules and stronger H bonding. In addition, the C=O stretching vibration band registered at 1798 cm^{-1} is more intense in the case of AV-loaded hydrogels, further confirming the successful integration of AV compounds into the GelMA matrix.

The evaluation of the ***antibacterial effects*** of the developed materials against Gram negative *E. coli* bacteria provided valuable insights into the potential design and applications of the composite hydrogels (Fig. 7).

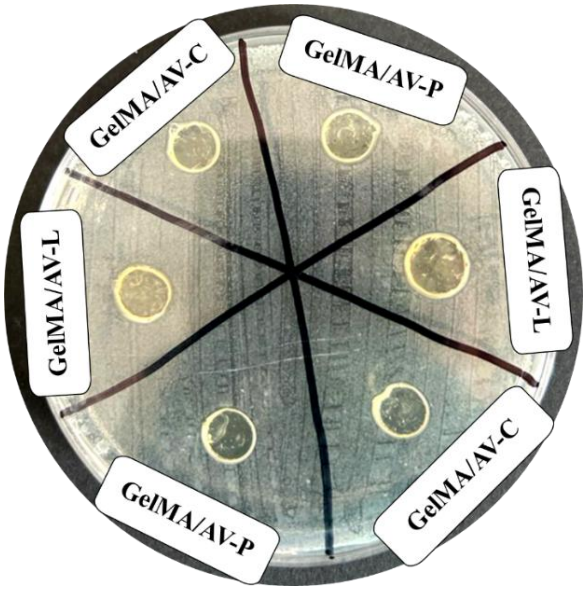

Fig. 7. Antibacterial effects of AV loaded hydrogels, showing the inhibition areas for control (GelMA/AV-C), powder-loaded (GelMA/AV-P) and lyophilized gel loaded samples (GelMA/AV-L).

The use of GelMA, a highly biocompatible material without inherent antibacterial properties, as a hydrogel matrix to incorporate low concentration of AV compounds determines a limited antibacterial response of the materials, as the matrix encapsulates the limited quantities of AV compounds and physically hinders their release from the hydrogel network in a non-hydrated medium. However, the limited bacterial growth induced by the AV-laden hydrogels, more notable in the case of GelMA/AV-L, is attributed to the incorporation of the extracted components. As the antibacterial activity of AV gel has been widely demonstrated [1, 2], our findings suggest the need of a synergistic approach towards enhancing the antibacterial effects of the composite hydrogels, underscoring the possibility of

tailored antibacterial effects through formulation adjustments. Further exploration of the observed effects holds promise for optimizing the therapeutic outcomes and advancing the design of such AV-loaded hydrogel-based biomaterials.

6. Conclusions

AV gel holds promising potential for tissue regeneration due to its rich bioactivity, encompassing numerous bioactive molecules. Our study aimed to exploit their synergistic activity by developing composite hydrogels loaded with AV compounds, using GelMA as a polymeric matrix. Characterization of extracted AV components favored the use of lyophilized AV gel over purified ACE for hydrogel fabrication. Incorporation of AV compounds, particularly lyophilized fibrous AV gel, significantly altered the properties of the formulations and of their resulting hydrogels, as confirmed by ATR-FTIR. The hydrogel network formation expressed as gel fraction was impacted significantly in the case of GelMA/AV-L. possibly due to larger pulp fibers intertwined between the polymeric chains during photopolymerization. The rheological assessment of the formulations indicated increased viscosity in GelMA/AV-L, which could be attributed to fibrous structures in the lyophilized gel inducing physical stabilization. A frequency dependency in the G' and G" of the hydrogels may be observed in the control sample, confirming the stabilizing effect of the AV compounds. Evaluation of the antibacterial effects show limited inhibition areas due to AV compound encapsulation within the three-dimensional polymeric network, with GelMA/AV-L showing improved potential for inhibiting bacterial growth against *E. coli*. The findings of the study highlight the potential of AV-loaded GelMA hydrogels as platforms for tissue regeneration, offering insights into the impact of AV compound incorporation on the natural hydrogel properties and paving the way for optimized therapeutic efficacy of these materials. Future research will focus on extensive testing of the synthesized hydrogels using multiple bacterial agents and bone-related cell lines to better understand their potential in bone tissue engineering.

Acknowledgement

This work was supported from the project *Integrating mechanically-tunable 3D printing with new bioactive multi(nano)materials for next functional personalized bone regenerative scaffolds*, PN-III-P4-PCE-2021–1240, no. PCE 88/2022.

REFERENCES

1. *M. H. Radha, N. P. Laxmipriya*, „Evaluation of biological properties and clinical effectiveness of aloe vera: A systematic review", Journal of Traditional and Complementary Medicine, **Vol. 5**, 2015, p. 21-6.

2. *A. A. Maan, A. Nazir, M. K. I. Khan, T. Ahmad, et al.,* „The therapeutic properties and applications of Aloe vera: A review", Journal of Herbal Medicine, **Vol. 12**, 1, 2018, p. 1-10.
3. *J. H. Hamman,* „Composition and applications of Aloe vera leaf gel", Molecules, **Vol. 13**, 8, 2008, p. 1599-616.
4. *N. Jittapiromsak, S. Jettanacheawchankit, P. Lardungdee, P. Sangvanich, et al.,* „Effect of acemannan on BMP-2 expression in primary pulpal fibroblasts and periodontal fibroblasts, in vitro study", Journal of Oral Tissue Engineering, **Vol. 4**, 3, 2006, p. 149-54.
5. *P. Chantarawaratit, P. Sangvanich, W. Banlunara, K. Soontornvipart, et al.,* „Acemannan sponges stimulate alveolar bone, cementum and periodontal ligament regeneration in a canine class II furcation defect model", Journal of Periodontal Research, **Vol. 49**, 2, 2013, p. 164-78.
6. *N. Jittapiromsak, S. Jettanacheawchankit, P. Lardungdee, P. Sangvanich, et al.,* „Acemannan, an extracted product from Aloe vera, stimulates dental pulp cell proliferation, differentiation, mineralization, and dentin formation", Tissue Eng Part A, **Vol. 16**, 6, 2010, p. 1997-2006.
7. *H. A. Trinh, V. V. Dam, W. Banlunara, P. Sangvanich, et al.,* „Acemannan Induced Bone Regeneration in Lateral Sinus Augmentation Based on Cone Beam Computed Tomographic and Histopathological Evaluation", Case Rep Dent, **Vol.**, 2020, p. 1-5.
8. *H. A. Trinh, V. V. Dam, B. Le, P. Pittayapat, et al.,* „Indirect Sinus Augmentation With and Without the Addition of a Biomaterial: A Randomized Controlled Clinical Trial", Implant Dent, **Vol. 28**, 6, 2019, p. 571-7.
9. *C. L. Van, H. P. T. Thu, P. Sangvanich, V. Chuenchompoonut, et al.,* „Acemannan induces rapid early osseous defect healing after apical surgery: A 12-month follow-up of a randomized controlled trial", J Dent Sci, **Vol. 15**, 3, 2020, p. 302-9.
10. *P. Jansisyanont, S. Tiyapongprapan, V. Chuenchompoonut, P. Sangvanich, et al.,* „The effect of acemannan sponges in post-extraction socket healing: A randomized trial ", J Oral Maxillofac Surg Med Pathol, **Vol. 28**, 2, 2016, p. 105-10.
11. *B. Rasoulian, A. Almasi, E. Hoveizi, Z. Bagher, et al.,* „Strong binding active constituents of phytochemical to BMPR1A promote bone regeneration: In vitro, in silico docking, and in vivo studies", J Cell Physiol, **Vol. 234**, 8, 2019, p. 14246-58.
12. *A. Y. Al-Hijazi, A. K. A. A. Al-Mahammadawy, E. I. Altememe,* „Expression of BMP7 in bone tissue treated with Aloe vera ", International Research Journal of Natural Sciences, **Vol. 3**, 2, 2015, p. 39-48.
13. *I. G. Kurian, P. Dileep, S. Ipshita, A. R. Pradeep,* „Comparative evaluation of subgingivally-delivered 1% metformin and Aloe vera gel in the treatment of intrabony defects in chronic periodontitis patients: A randomized, controlled clinical trial", J Investig Clin Dent, **Vol. 9**, 3, 2018, p. 1-8.
14. *F. Yang, P.-w. Yuan, Y.-Q. Hao, Z.-M. Lu,* „Emodin enhances osteogenesis and inhibits adipogenesis", BMC Complement Altern Med, **Vol. 14**, 1, 2014, p. 74.
15. *S. Rahman, P. Carter, N. Bhattarai,* „Aloe Vera for Tissue Engineering Applications ", J Funct Biomater, **Vol. 8**, 1, 2017, p. 6-16.
16. *Y. Matsumoto, Y. Tousen, Y. Ishimi,* „β-Carotene prevents bone loss in hind limb unloading mice", J Clin Biochem Nutr **Vol. 63**, 1, 2018, p. 42-9.
17. *B. Lv, L. Lu, L. Hu, P. Cheng, et al.,* „Recent advances in GelMA hydrogel transplantation for musculoskeletal disorders and related disease treatment", Theranostics, **Vol. 13**, 6, 2023, p. 2015-39.
18. *M. Sun, X. Sun, Z. Wang, S. Guo, et al.,* „Synthesis and Properties of Gelatin Methacryloyl (GelMA) Hydrogels and Their Recent Applications in Load-Bearing Tissue", Polymers (Basel), **Vol. 10**, 11, 2018, p. 1290.

19. *K. Yue, G. T.-d. Santiago, M. M. Alvarez, A. Tamayol, et al.,* „Synthesis, properties, and biomedical applications of gelatin methacryloyl (GelMA) hydrogels", Biomaterials, **Vol. 73**, 2015, p. 254-71.
20. *A. C. Daly, P. Pitacco, J. Nulty, G. M. Cunniffe, et al.,* „3D printed microchannel networks to direct vascularisation during endochondral bone repair", Biomaterials, **Vol. 162**, 2018, p. 34-46.
21. *X. Zhao, S. Liu, L. Yildirimer, H. Zhao, et al.,* „Injectable Stem Cell-Laden Photocrosslinkable Microspheres Fabricated Using Microfluidics for Rapid Generation of Osteogenic Tissue Constructs", Advanced Functional Materials, **Vol. 26**, 17, 2016, p. 2809-19.
22. *B. Byambaa, N. Annabi, K. Yue, G. T.-d. Santiago, et al.,* „Bioprinted Osteogenic and Vasculogenic Patterns for Engineering 3D Bone Tissue", Advanced Healthcare Materials, **Vol. 6**, 16, 2017, p. 1700015.
23. *B. Zhou, X. Jiang, X. Zhou, W. Tan, et al.,* „GelMA-based bioactive hydrogel scaffolds with multiple bone defect repair functions: therapeutic strategies and recent advances", Biomaterials Research, **Vol. 27**, 86, 2023, p. 1-15.
24. *A. I. V. D. Bulcke, B. Bogdanov, N. D. Rooze, E. H. Schacht, et al.,* „Structural and Rheological Properties of Methacrylamide Modified Gelatin Hydrogels", Biomacromolecules, **Vol. 1**, 2000, p. 31-8.
25. *S. Kumar, A. B. Tiku,* „Immunomodulatory potential of acemannan (polysaccharide fromAloe vera) against radiation induced mortality in Swiss albino mice", Food and Agricultural Immunology, **Vol. 27**, 1, 2015, p. 72-86.
26. *Z. X. Lim, K. Y. Cheong,* „Effects of drying temperature and ethanol concentration on bipolar switching characteristics of natural Aloe vera-based memory devices", Physical Chemistry Chemical Physics, **Vol. 17**, 40, 2015, p. 26833-53.
27. *S. S. Namazi, A. H. Mahmoud, R. Dal-Fabbro, Y. Han, et al.,* „Multifunctional and biodegradable methacrylated gelatin/Aloe vera nanofibers for endodontic disinfection and immunomodulation", Biomaterials Advances, **Vol. 150**, 2023, p. 1-11.
28. *A. I. Cernencu, G. M. Vlasceanu, A. Serafim, G. Pircalabioru, et al.,* „3D double-reinforced graphene oxide – nanocellulose biomaterial inks for tissue engineered constructs", RSC Advances, **Vol. 13**, 34, 2023, p. 24053-63.
29. *R. L. Alexa, H. Iovu, B. Trica, Catalin Zaharia, et al.,* „Assessment of Naturally Sourced Mineral Clays for the 3D Printing of Biopolymer-Based Nanocomposite Inks", Nanomaterials **Vol. 11**, 3, 2021, p. 703.
30. *W. Wang, Y. Zhu, Y. Liu, B. Chen, et al.,* „3D bioprinting of DPSCs with GelMA hydrogel of various concentrations for bone regeneration", Tissue and Cell, **Vol. 88**, 2024, p. 102418.
31. *E. Olăreț, D. Steinmüller-Nethl, H. Iovu, I.-C. Stancu,* „Nanodiamond Loaded Fish Gelatin Enzymatically Crosslinked Hydrogels", UPB Sci Bull, Series B, **Vol. Vol. 84**, 3, 2022, p. 125-36.
32. *D. F. S. Fonseca, P. C. Costa, I. F. Almeida, P. Dias-Pereira, et al.,* „Swellable Gelatin Methacryloyl Microneedles for Extraction of Interstitial Skin Fluid toward Minimally Invasive Monitoring of Urea", Macromolecular bioscience, **Vol. 20**, 10, 2020, p. e2000195.
33. *M. Ibrahim, A. A. Mahmoud, O. Osman, M. A. El-Aal, et al.,* „Molecular spectroscopic analyses of gelatin", Spectrochimica acta Part A, Molecular and biomolecular spectroscopy, **Vol. 81**, 1, 2011, p. 724-9.